TRUST

High resolution monitoring, real time visualization and reliable modeling of highly controlled, intermediate and up-scalable size pilot injection tests of underground storage of CO_2

Contract #309067

Deliverable Number	**D4.2**
Title	**Approaches for Large Scale Modeling**
Work-Package	**4**
Lead Participant	**IIT**
Contributors	**CSIC, UU, IMPCOL, EWRE**
Version:	**1**
Revision level:	**01**
Due Date:	**Month 36**
Reviewed by:	
Status:	
Dissemination level	**PU**

Executive summary

The understanding of the modeling methodology and the techniques for the long term and industrial scale behavior of the CO_2 storage is necessary to face the required model predictions for the future projects. In this deliverable of task 4, we collect the most efficient existing numerical applications at large scales, in order to model the long-term and large-scale behavior of CO_2 injection, as part of WP10, needed to develop industrial scale application.

This deliverable includes a brief description of the nature of the CO_2 storage as a physical phenomenon to understand properly the processes that occur at small scales but may have to be included for modeling the large scales. Large scale modeling is essentially a two dimensional exercise because horizontal extent on aquifers lies in the range of 10s to 100s km, whereas vertical extent ranges in the 10s to 100s m, leading to aspect ratios around 1000. Yet, many of the processes that are relevant (e.g. buoyancy or dissolution) occur along the vertical direction. Therefore, it is not surprising that specific methods have been developed to handle these processes. In fact, numerical approaches have been developed for years in the context of multiphase flow applications, so that there is a broad range of codes available. For the purpose of facilitating description, numerical techniques have been separated in three groups. The first one includes standard numerical codes that solve the traditional multiphase flow equations, possibly coupled to energy conservation, reactive transport and/or mechanical equilibrium. The second group includes the vertical equilibrium (VE) models, which explicitly integrate along the vertical direction to reduce the dimensionality of the problem. The last group refers to semi-analytical solutions useful to approximate large scale models (e.g., through superposition of well hydraulics solutions) or used to include specific features or processes (e.g., flow to a well or CO2 dissolution) into existing numerical simulators to catch such processes in an efficient manner. In spite of the advances in the standard modeling methods (first group above), we conclude that the vertical equilibrium (VE) models can run large scales models gaining efficiency without missing the relevant small scale processes, included through semi-analytical approaches.

Keywords	Large scales, Long-term, small scale multiphase processes, CO_2 injection, CO_2 storage, vertical equilibrium models, semi-analytical solutions, standard numerical method for multiphase flow, basin-scale storage capacity estimation workflow, injection strategies, geomechanical response.

Table of Contents

1. Introduction

This deliverable summarizes modeling methodologies that are appropriate for studying the long term behavior of CO_2 to be injected at industrial scale sites. Actual industrial scale models will be presented as part of WP10, which will require site specific models and enhanced parameter estimation approaches. It is also related to the experimental sequences developed in WP02 (see tasks 2.5 and 2.6) where the activities design of this deliverable are translated into practical steps in the field, determining the timing of each experimental stage, the needed logistics for the injection, the monitoring and the onsite sampling and chemical analysis and handling of the data acquisition systems.

The assessment of modeling methodologies included in this deliverable will be carried out by studying the phenomena involved in CO_2 storage and the influence of small scale processes at the regional scale. Focusing on this influence over the complexities at large scale simulations where is relevant the study of the pressure build-up, pressure plume, risk of CO_2 escape, pollution of adjacent water bodies etc. For that propose, we describe the existing simulators and their modeling approaches to model large scale CO_2 storage. We also introduce a detailed overview of the vertical integration approach which looks like the most efficient approach to model the large scale long-term simulations and the concept of the basin-scale storage capacity estimation workflow, suitable for the evaluation of storage potential of a given target site. Finally, we show some small preliminary applications that have been carried out so far.

2. The phenomenon

2.1 The CO_2 injection during the geological CO_2 storage

Geological storage involves injecting CO_2 in deep reservoirs (Figure 4.1), which are suitable geological formations, such as porous and permeable rock. Reservoirs must be covered by a caprock that prevents the escape of CO_2 to the surface. CO_2 is stored at depth to ensure an optimal use of the pore space available for storage. Hence, most of CO_2 storage projects (*Taber*, 1994; *Korbul and Kaddour*, 1995) assume injection depths of more than 800m and pressures of more than 80 bars to guarantee a high density.

Geological storage of CO_2 includes two stages: Injection stage and post-injection/migration stage.

The *injection phase* begins by injection CO_2 from one or more sources into the reservoir. This produces the displacement of the resident brine and the increment of the pressure build-up near the wellbore zone. The pressure build-up could also be increased by the entry pressure due to capillarity in a lower level. The physical description of this displacement is defined by momentum conservation, in which both phases (non-wetting phase, CO_2 (supercritical) and wetting phase, brine) move with the same motion. CO_2 tends to move upward due to density factor between both fluids.

The additional pressure produced by the displacement may deform the rock matrix of the formation with changes in matrix porosity or fracture apertures. They in turn cause changes in flow permeability and, consequently, the flow field. This is what we call the hydromechanical effect. In this phase, the driving forces include: buoyancy flow of the CO_2 with its factor-of-two lower density, which dominates far from the well, and viscous flow which dominates near the well with an order-of-magnitude lower viscosity for the CO_2. For example, for storage of CO_2 at 1,000 m depth, CO_2 density is about 60–75% that of water in the formation, while its viscosity is about a factor of 15–20 times less than that of water (Figure 2.1(a)).

The *Post-injection stage* begins when injection stops. After injection ceases, pressure build-up in the storage formation dissipates and CO_2 is subject only to background flow and buoyancy as the driving mechanism for flow. From this moment, plume migration is divided into two parts, an immobile part which is a residual zone due to the push of the wetting phase over the non-wetting saturated pores (residual trapping) and a mobile plume which moves as far as it reaches pressure dissipation into the reservoir. This leads to a slow migration of the CO_2 plume into the reservoir. Figure 2.1(b).

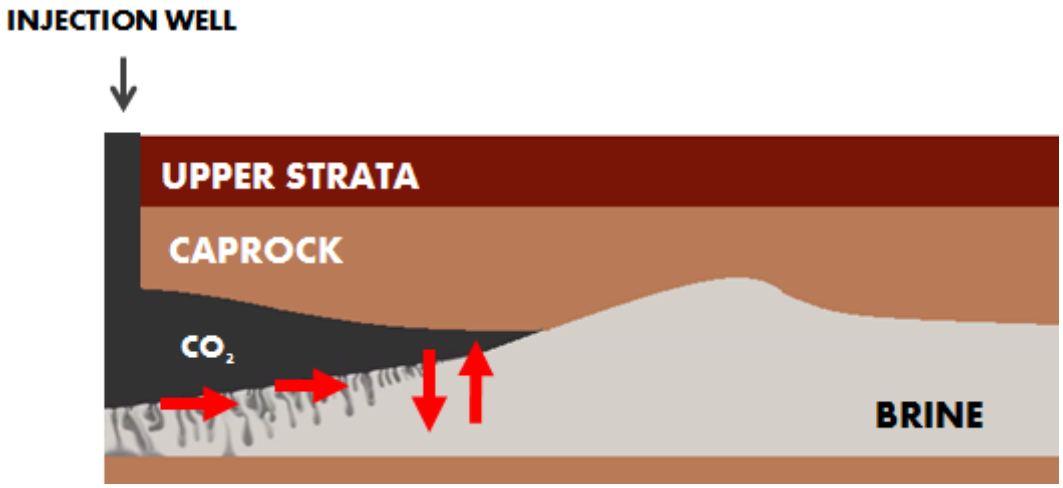

Figure 2.1(a): Schematic diagram of CO_2 geo-sequestration in saline formation during injection phase. Driving forces are performed by red arrows (viscous forces by horizontal arrows and buoyancy forces by vertical arrows).

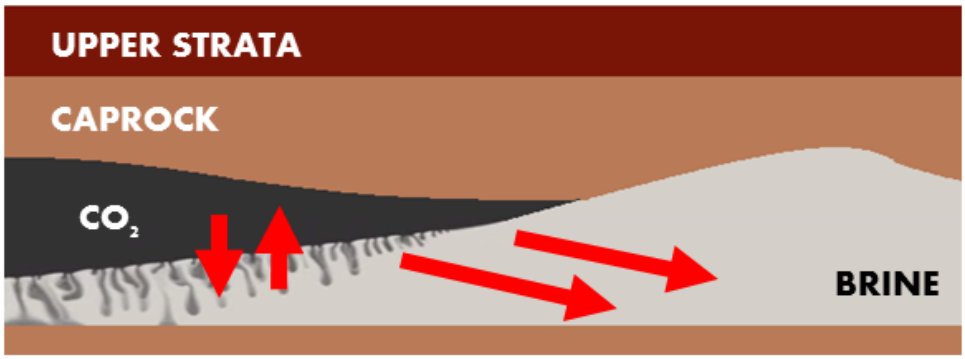

Figure 2.1(b): Schematic diagram of CO_2 geo-sequestration in saline formation during post-injection phase. Driving forces are performed by red arrows (buoyancy forces by vertical arrows and regional flow by sloped arrows).

The models of the CO_2 are based in processes. Both stages mentioned include different small scale multiphase processes which have to be defined with accuracy. In the following we will explain the nature of the CO_2 behavior and its influence over the processes.

2.2 Multiphase processes at the large scales of the CO_2 storage

The nature of the CO_2 under storage conditions is essential to understand the processes. First, we will introduce the CO_2 behavior. CO_2 injected into a deep brine formation will be present in three forms: a dense supercritical gas phase, a dissolved state in pore water, and an immobilized state through geochemical reaction with in situ minerals. The dissolved part of CO_2 storage is estimated to be from 2% in saturated NaCl brines by weight to 7% in typical groundwater. CO_2 immobilization in formation matrix minerals is a slow process and varies considerably with rock types. The amount of CO_2 sequestered through such mineral reactions can be comparable with CO_2 dissolution in pore waters. Among all the forms that the injected CO_2 takes in a brine formation, the supercritical gas phase is the main storage form and it has properties quite different from those of the pore water.

The difference of densities between stored supercritical CO_2 and the resident brine yields a CO_2 buoyancy flow to the top of the injection zone below the caprock. This buoyant flow of CO_2 is also affected by the vertical and horizontal permeabilities of the aquifer. The buoyancy of CO_2 is relevant during large scale modeling due to the areal extent of the injected CO_2 will be much larger than a buoyancy-neutral fluid. For example, storage of 2.7 x 1010 kg of CO_2, injected at a rate of 350 kg/s for 30 years into a 100-m thick formation with $k_x = k_z = 10\text{-}13$ m^2, has been estimated to have an increase in areal extent resulting from buoyancy flow by a factor of approximately between 12-16. In this example, because of the large volume of CO_2 involved, the areal extent of the supercritical gas in the injection zone can be as much as 600 km^2.

The upward CO_2 flow in the aquifer is vertically limited by the low permeability and mainly by the high gas entry pressure of the caprock. One can estimate the thickness of the layer of CO_2 needed to provide enough buoyancy pressure to exceed the gas entry, which is 70-170 m for a pore radius of 10e-7 m. However, if the CO_2 plume finds a path of leakage in the caprock, such as fracture or fault, the effective pore radius in the fracture can be much larger and thus the thickness of CO_2 required to overcome the gas entry pressure of the fracture would be much less. The CO_2 could also leak out of the reservoir if it finds an abandoned well.

Because of the large volume of CO_2 injected and stored, the displacement of in situ brine is also an issue of concern. The displaced brine may migrate to neighboring formations and/or diffused into shallower hydraulically conductive units. Potential focused migration may also occur through abandoned wells or sub-vertical faults and connected fractures. Moreover, brine could leak through the caprock due to the absence of capillarity barrier. Its flow which is controlled by the build-up reached in the reservoir only is limited by the low permeability. Hence, brine migration through the caprock and through the upper strata could be huge. In order to quantify: For example, in a reservoir with a thicknesss of 100m, with an intrinsic permeability of 1e-18 m2 (10e-12 m/s of hydraulic conductivity for brine aprox.) and with a gradient of pressure of 10, the brine leakage flow is about 3200 m3/km2/year. Hence, if we inject CO_2 during 30 years the volumetric amount of brine displaced through the upper strata in areal extent of 500 km2 is about 30 Mtn.

Other parameter which affects to the CO_2 flow is the very low viscosity of its supercritical state. The supercritical CO_2 viscosity will give rise to flow instability at the CO_2-brine interface as CO_2 is being injected into the storage formation. This flow instability results in fingering. In other words, instead of piston-like flow of the CO_2 front into the injection formation, parts of the front will flow much faster in the form of fingers. This phenomenon occurs in parallel with the buoyancy flow effect discussed above.

However, viscous fingering of CO_2 may not be as significant in the presence of geologic heterogeneity. Heterogeneity of the injection formation gives rise to the fingering or channeling effect. The injected CO_2 will be channelized to follow the most permeable paths because of the spatial variation of permeability. The flow pattern will depend not only on the permeability variability and its spatial correlation range, but also on the saturation level of CO_2 in the different parts of the brine formation.

It will be also relevant evaluate the pressure build-up generated in the reservoir. Mechanically, it is necessary to ensure the well integrity and hydraulic fracturing by limiting the injection and buoyancy pressures induced in the reservoir. While injection pressure is highest around the injection well and starts to decrease after the termination of injection, buoyancy pressure extends over the entire CO_2 plume and lasts well beyond the injection period. An increase in formation fluid pressure, due to both injection and buoyant pressures, will lead to local changes in the effective stress field, which, in turn, will induce mechanical deformations, possibly increasing the porosity and permeability and thus reducing the fluid pressure. However at the same time, increasing pressure may also cause irreversible mechanical failure in the caprock. This mechanical failure may involve possibly shear-slip along existing fractures and creation of new fractures (hydraulic fracturing), that reduce the sealing properties of the caprock system. In addition to these mechanical processes, replacing the native formation fluid with CO_2 may cause changes in rock mechanical properties through chemo-mechanical interactions between the CO_2 and the host rock, or through desiccation of fractures.

Chemically, at the CO_2 front where CO_2 is dissolved in water, the acidity of the groundwater is increased and many minerals comprising the host rock matrix minerals such as calcite, may dissolve readily, leading to an increase in permeability and porosity along the flow channel. This leads to a higher flow rate and increased dissolution, potentially forming what are known as wormholes. On the other hand, based on experience from enhanced oil recovery, CO_2 has been known to reduce injectivity in some cases, but to increase permeability near injection wells in others. There are also data indicating that dissolved CO_2 will cause a reduction in permeability where the carbonate minerals precipitate along the flow paths with a large pressure gradient. All these observations suggest the need for careful evaluation of the compatibility between supercritical CO_2 and geochemistry of the brine formation. Such an evaluation may also yield information useful for the design of injection operations, such as keeping injection pressure below a certain value so that there will be no severe pressure gradients to induce precipitation or dissolution.

So far we have done a general review of the phenomenon over the time. As we can see above, this implies several processes which have been studied during years for other applications in porous media, such as geothermal energy, petroleum industry, or storage of hazardous materials. These applications involve a number of phenomena, including multiphase flow (*Olivella et al.*, 1996; Wheeler et al, 2001; *Pruess et al.*, 2004; *Flemisch et al.*, 2007; Schlumberger, 2007; *Gasda et al*, 2009; *Møll Nilsen et al,* 2015), geomechanical and geothermal effects (*Walsh*, 1981; *Cook*, 1992; *Olivella et al.*, 1996; *Spycher and Pruess*, 2009), and geochemical processes (*Parkhurst et al.*, 1999; *Xu and Pruess*, 2001; *Xu et al.*, 2006; *Steefel*, 2009).

The recent literature on Geological Carbon Storage (GCS) is extensive and covers a broad range of approaches: experimental works (*Palandri et al.*, 2005; *García-Rios et al.*, 2013), multiphase simulations including geomechanics at Darcy scale (*Rutqvist et al.*, 2002; *Bauer et al.*, 2012; *Helmig et al.*, 2013) or also about monitoring real cases (*Estublier and Lackner*, 2009; *Eiken et al.*, 2011). Most of them have been developed by using tools built in the past for others purposes. Also relevant is to address impacts over different trapping strategies in order to enhance storage security (*Hesse et al.*, 2009; *Hidalgo et al.*, 2013). Thus, the final goal of this technology is the achievement of an efficient and secure CO_2 storage.

3. Approaches

This section gives a brief overview of some current simulators available to model large scales of CO_2 storage. There are three different ways to carry out simulations of the large scale of the CO_2 storage. We include these three approaches separating in groups. First one is formed by the standard numerical codes. Second group includes the vertical equilibrium models. Both groups have a brief code description of the each simulator. The last group refers to semi-analytical solutions useful to simulate large scale models as well or used to be included into some codes to catch some process more efficient than in case of numerical models.

3.1 Standard simulators (full 3D).

This section is based on a collection of some of the current existing tools to model CO_2 storage from the numerical standard approach.

3.1.1 Dumux

DuMux is a free and open-source simulator for flow and transport processes (*Flemisch et al*, 2007). It is based on the Distributed and Unified Numerics Environment Dune. For the simulation of CO_2 injection scenarios, DuMuX is based on a two-phase two-component flow model using a fluid system considering a gaseous (CO_2) and a liquid phase (brine) with mutual miscibility. The equations of the model can spatially be discretized by a vertex-centered finite volume (box) method (*Helmig*, 1997) or a cell-centered finite volume scheme, while time discretization is realized by an implicit Euler scheme. It has been used in long term models of the CO_2 injection (*Class et al*, 2009).

On top of that, the "ElTwoP"-model in DuMuX implements two-phase flow of compressible immiscible fluids in a deforming matrix. In addition to the equations for two phase-flow (spatially discretized by the box method), it solves a quasi-stationary momentum balance equation of the porous medium using a Standard Galerkin Finite Element scheme. The influence of the pore fluid on the on the deformation of the matrix is accounted for through the effective stress concept (Biot 1941). The feedback of the deformation on the flow is introduced via the effective porosity and effective permeability which are functions of the solid displacement. All equations are solved fully coupled.

3.1.2 ECLIPSE

ECLIPSE is a simulation tool used extensively in the oil and gas industry (*Schlumberger*, 2007). It could be a robust choice in the large scales of CO_2 simulations. It comprises 2 software packages: ECLIPSE Black Oil (E100) and ECLIPSE Compositional (E300). ECLIPSE BlackOil (E100) is a fully implicit, three-phase, 3D, general-purpose black oil simulator. ECLIPSE Compositional (E300) is a compositional simulator with a cubic equation of state, pressure-dependent permeability values and black oil fluid treatment. Different options have been implemented in E300 to handle CO_2 solubility in water. Also it has the capability of accurately computing the physical properties (density, viscosity, compressibility, etc.) of pure and impure CO2 as a function of temperature and pressure. Moreover, it includes CO2SOL which was developed to model CO_2 enhanced oil recovery and it includes also a tool to add gas components, such as CH4 and H2S in case of gas depleted reservoirs. ECLIPSE has been applied by a group from Schlumberger Carbon Services and by a group from Heriot-Watt University, Edinburgh.

3.1.3 TOUGH2

The simulation code TOUGH2 was developed by Lawrence Berkeley National Laboratory (*Pruess et al*, 1999). TOUGH2 is a general-purpose simulation code for non-isothermal flows of multi-component, multi-phase fluids in porous and fractured media. TOUGH2 is written in standard FORTRAN77. It is used in CO_2 storage by years. Numerically, the spatial discretization employs integral finite differences, while time is discretized in a fully implicit way using first-order finite differences. TOUGH2 numerical simulations for CO_2 storage employs the equation-of-state module ECO2N. It describes the thermodynamics and thermophysical properties of H_2O - NaCl - CO_2 mixtures, and accurately reproduces fluid properties for the temperature, pressure and salinity conditions of interest for geological sequestration. If far-field pressure and brine migration is of concern, single-phase simulations using TOUGH2 can be conducted, which significantly reduces the computational time. TOUGH2/ECO2N accounts for the complex thermodynamics of supercritical CO_2 injection and migration in saline aquifers.

3.1.4 IPARS-CO2

The code IPARS-CO2 within the compositional model of the simulator IPARS (*Wheeler et al*, 2001) is being developed and maintained by the Center for Subsurface Modeling (CSM) at the University of Texas at Austin. It can treat non-isothermal compositional flow equations in parallel. Also it has two-phase immiscible flow models, a black-oil model and flow coupled to reactive transport, among others. It is suitable for multiphase simulation, included large scales CO_2 storage. Numerical method used is an iteratively coupled implicit pressure, explicit concentrations (IMPEC) sequential algorithm is applied to enforce the non-linear saturation constraint and a time split method is employed to solve thermal energy balance with a higher-order Godunov method for advection and a fully implicit mixed FEM for conduction. The thermal and flow steps are sequentially coupled.

3.1.5 CODE_BRIGHT

CODE_BRIGHT is a Finite Element Method (FEM) program capable of performing coupled thermo-hydro-mechanical (THM) analysis in geological media (*Olivella et al*, 1996). It has been developed at the Polytechnic University of Catalonia (UPC), and works combined with the pre/post-processor GiD, developed by the International Center for Numerical Methods in Engineering (CIMNE). It employs the compositional approach for multiphase flow problems. It has been used for CO_2 storage (*Vilarrasa et al*, 2013).

3.1.6 PFLOTRAN

PFLOTRAN is an open source, massively parallel subsurface flow and reactive transport code (*Peter et al*, 2015). It solves a system of generally nonlinear partial differential equations describing multiphase, multicomponent and multi scale reactive flow and transport in porous materials. The choice to use PFLOTRAN for this report is due to its ability to simulate large models quickly along with its dedicated approach to CO_2 sequestration. The mode used for the simulations is MPHASE, which solves a non-isothermal 2 phase flow (gas and liquid), energy and transport models. The MPHASE flow model has 2 components (CO_2 and H_2O) miscible in all proportion in both phases, while the liquid phase only could have other components. This tool has been employed at the application of the injection strategies from this deliverable.

3.1.7 THE ICGT Library

The IC Geomechanics Toolkit (ICGT) is a finite element-based discrete fracture and fault propagation simulator, in which deformation is numerically computed based on measurable material properties, such as Young's modulus and Poisson's ratio, using an arbitrarily generated tetrahedral mesh. Fractures and faults are represented discretely using surfaces and curves, and are represented as discontinuities in the flow field, which allows modelling the flow within fractures independently and in combination with flow within the matrix. This approach is unique, in that fracture and fault geometry is stored independently from the mesh, and so fracture growth is not restricted to conform to an existing mesh, nor is it constrained by the mesh. The finite element method is used to compute the deformation and flow in the system, taking into account the deformation of the material, the fracture surface geometry and topology, and the fluid flow through the discontinuities. The ICGT heavily interacts with CSMP++ (Complex Systems Platform), an object-oriented finite-element based library that is specialised in simulating complex multi-physics processes, a multi-institutional code (main contributors: Imperial College, Heriot Watt, ETH Zürich, Montan University, Melbourne University) that has been extensively validated to model transport, single-phase and multiphase flow, as well as reactive transport and heat transfer, in fractured media in two and three dimensions, against both experimental and field experiments, and that can run on workstations as well as on high performance computing systems. This tool has been employed at the application geomechanical response from this deliverable.

3.2 Vertical equilibrium frameworks

This section includes existing tools to model CO_2 storage based integrating the flow equations along the vertical direction. In practice, this entails assuming vertical equilibrium (VE), at least for hydrodynamics. Details about VE models are presented in the section 4.

3.2.1 VESA: Vertical Equilibrium with Sub-scale Analytical method

It has been developed at Princeton University and it is based on the Vertical Equilibrium concept proposed by *Gasda et al*, 2009. It combines a numerical vertical-equilibrium aquifer model with an embedded analytical solution for wellbore flow in cases where leaky wells are present in the system. Hence is focus on the study of the large scale injection of CO_2 and specially, in the study of large uncertainties associated to CO_2 leakage through a well. Formulation has been explained in detail on section 4.3. Numerically, the set of equations is solved by a standard cell-centered finite-difference approximation using the IMPES approach, also explained previously. The timestep used in the explicit (transport) step is controlled by a CFL condition. It is efficiently employed in many models of long term CO_2 storage (*Class et al*, 2009).

3.2.2 MRST/CO2lab

The Numerical CO_2 Laboratory is a Matlab Reservoir Simulation Toolbox (MRST) module. MRST is an open-source framework developed by SINTEF (*Møll Nilsen et al*, 2015a). CO2lab module allows simulate the large-scale and long-term CO_2 storage and study the effects of the structural, residual and solubility trapping over long time periods. Numerical method used by the module is the fully-implict method with phase-based upstream-mobility weighting and two-point flux approximation. In the recent years, it has

been modeled a bench of small models and some other models from pilot projects (*Møll Nilsen et al*, 2015a, 2015b).

3.3 Semi-analytical solutions for pressure build-up and CO_2 plume evolution

Industrial-scale CO_2 injection may lead to large pressure build-up and significant far-field brine migration as well as their associated geomechanical and hydrogeological impacts, which may become a limiting factor for the CO_2 storage capacity. It is therefore necessary to carefully study the evolution and impact of the pressure plume and brine migration (see section 2.2). In this section, we summarize the methodologies developed for the estimation of near-well and far-field pressure buildup, based on existing or extended numerical approaches and (semi)-analytical solutions.

For a typical industrial-scale CO_2 injection scenario, there exist a dry-out zone (free of water) around the injection well (see Figure 3.1). In this dry-out zone all water has been either displaced outwards or vaporized into the CO_2 rich (gas) phase and the salt that was originally dissolved in the brine has precipitated. The radius of dry-out zone is typically on the scale of ~10^2 meters at the end of the injection period. Surrounding the dry-out zone is a region where the gas phase and the aqueous phase coexist. The radius of this two-phase flow region is typically several kilometers at the end of the injection period. Outside of the two-phase region only brine exists with single-phase brine flow, and we refer to this region as the far-field.

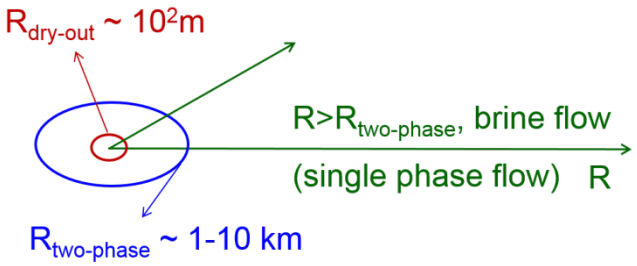

Figure 3.1: Schematic of spatial scales relevant for pressure evaluation

When estimating of the far-field pressure buildup, the simplification of assuming single-phase flow may be made, due to the fact that two-phase flow effect is relatively local (within a few kilometres from the well). With this simplification, the Theis solution for pressure buildup ΔP at radial distance r and time t for an ideal aquifer, is

$$\Delta P = P - P_{ini} = \frac{Q\mu_b}{4\pi kb}\int_u^\infty \frac{e^{-u}}{u}du \qquad \text{Eq. 3.1}$$

Where,

$$u = \frac{r^2 S\mu_b}{4tk\rho_b gb} \qquad \text{Eq. 3.2}$$

In eqs. (3.1-3.2), P is the vertically averaged pressure, P_{ini} is the initial pressure (vertically averaged), Q is the volumetric injection rate, k is the permeability of the reservoir, S is the storativity of the reservoir, b is the thickness of the reservoir, ρ_b is the density of the native brine, μ_b is the viscosity of the brine.

Storage aquifer may have a caprock layer with permeability that is not sufficiently low to constrain brine leakage but functions as a capillary barrier for the non-wetting CO_2 phase. In this leaky-aquifer case, the Theis solution can be replaced by the Hantush and Jacob solution. For a reservoir bounded by cemented (impermeable) faults, the method of images may be used for the analytical calculations to take into account the effect of no-flow and constant pressure boundaries.

When the near-well pressure buildup is of concern, one needs a two-phase flow based semi-analytical approach. Approximate solutions are provided by Mathias et al. (2010), and Vilarrasa et al. (2011, 2014). The simplest of these consists of assuming vertical pressure equilibrium, constant fluid properties, negligible capillary pressure and equilibrium dissolution between CO_2 and water, *Mathias et al*, 2010, solved the relevant (radially symmetric) governing equations describing the above flow characteristics. The semi-analytical solution can be applied to both laterally open and closed aquifers. It is summarized as follows.

$$\Delta P = P - P_{ini} =$$
$$\frac{M_0}{4\pi\rho_g Hk}\begin{cases}\mu_g q_{D1}\ln\left(z_T/z\right)/k_{rs} + \mu_g q_{D2}F_2\left(z_T\right) + \mu_b q_{D3}F_1\left(z_L\right), & 0 \le z < z_T \\ \mu_g q_{D2}F_2\left(z\right) + \mu_b q_{D3}F_1\left(z_L\right), & z_T \le z < z_L \\ \mu_b q_{D3}F_1\left(z\right), & z \ge z_L\end{cases} \qquad \text{Eq. 3.3}$$

where M_0 is the mass injection rate of CO_2, ρ_g is the density of CO_2, μ_g is the viscosity of CO_2, k is the permeability of the formation, H is the thickness of the formation, k_{rs} is the permeability reduction factor due to salt precipitation, μ_b is the viscosity of the brine, q_{D1}, q_{D2}, and q_{D3} are the dimensionless, piecewise total fluxes, which can be obtained from Equations (27) and (28) in *Mathias et al*, 2010, z is the similarity transform variable for time t and radial distance r

$$z = \frac{\pi\phi\rho_g Hr^2}{M_0 t} \qquad \text{Eq. 3.4}$$

and z_T and z_L are locations of the trailing and leading shocks in similarity space. In Equation 3.3,

$$F_1\left(z\right) = \begin{cases}\left(\alpha z_E\right)^{-1} - \frac{3}{2} + \ln\left(\frac{z_E}{z}\right) + \frac{z - z_L}{z_E}, & z_E < \frac{0.5615}{\alpha} \\ E_1\left(\alpha z\right), & z_E > 0.5615/\alpha\end{cases} \qquad \text{Eq. 3.5}$$

$$\alpha = \frac{M_0\mu_b\left(c_r + c_b\right)}{4\pi\rho_g Hk} \qquad \text{Eq. 3.6}$$

With

$$F_2(z) = -\frac{1}{\mu_g}\int_z^{z_L}\left(\frac{k_{ra}}{\mu_b}+\frac{k_{rg}}{\mu_g}\right)^{-1}\frac{1}{z}dz \qquad \text{Eq. 3.7}$$

Where z_E is similarity transform for the radial extent of the formation r_E, k_{ra} and k_{rg} are the relative permeabilities of the aqueous phase and gas phase, respectively, and c_r and c_b are the compressibilities of rock pores and brine, respectively.

To account for the effect of closed boundaries, we introduce imaginary injection wells to calculate the additional pressure increase due to the no-flow boundaries. The additional pressure increase (ΔP_f) is calculated as:

$$\Delta P_f = \sum_{i=1}^{n_{im}} \Delta P_i(r_i, t) \qquad \text{Eq. 3.8}$$

Where n_{im} is the number of imaginary injection wells, and $\Delta P_f(r_i,t)$ is the pressure buildup contribution (calculated by Equation 3.1) from the ith imaginary well with a distance r_i from the actual injection well. The superposition of image well solutions can also be applied to the analytical solution for single-phase flow (Eq. 3.1).

Existing analytical and most numerical solutions to this problem assume that the injection takes place uniformly along the whole thickness of the aquifer (Nordbotten et al. 2005; Nordbotten and Celia 2006; Dentz and Tartakovsky 2009a; Vilarrasa et al. 2010a). This assumption is unrealistic because of buoyancy. Also, they have not included the CO_2 compressibility effects. The effects of the buoyancy difference between fluids and CO_2 compressibility on the long-term simulations are relevant, as it includes the second chapter of this deliverable. *Vilarrasa et al.* (2013) develops a semi-analylical solution for the CO_2 plume shape and the pressure evolution. This solution includes the CO_2 compressibility and buoyancy in the well. It also acknowledges that CO_2 flux into the aquifer is not uniform along the aquifer thickness. The solution was developed and programmed in a spreadsheet by Vilarrasa and it can be downloaded from GHS (2012).

The extent and the thickness of the CO_2 plume as well as the overpressure can be quickly assessed. He formulates the problem and presents the methodology for solving it when the CO_2 mass flow rate or the CO_2 pressure is prescribed at the injection well. Finally, he presents an application of this methodology and compares the results with full numerical simulations.

Because of their simplicity, the analytical and semi-analytical solutions may not be generally applicable to situations where the assumptions were not met. If this is the case, the more versatile numerical approaches can be used (first and second group of this chapter).

4. Vertical integration models

The classic approach to modeling CO_2 storage employs fully 3D numerical methods to achieve a high degree of accuracy. At large spatial and temporal scales, 3D models are computationally expensive and prohibitive. Specially, if there are small scale phenomena, such as the injection area, leakage through abandoned wells or convection-dissolution process, which require a fine mesh.

One solution could be to upscale the phenomena in order to simplify calculations, without losing accuracy. This requires an accurate knowledge of time and spatial scales of the dominating processes. Here we will simplify the governing equations by means of upscaled models based on the assumption of Vertical Equilibrium (VE).

The VE models have been subject to study in porous media in recent times (*Bear*, 1999; *Sorek et al.*, 2001; *Bakker*, 2003; *Pool et al.*, 2011) and have been developed by petroleum industry for systems such as layered reservoirs and strongly vertically segregated flow (*Dietz*, 1953;*Martin*, 1958; *Coats et al.*, 1967, 1971; *Yortsos*, 1995). One of advantages of the CO_2-brine system is that it is simpler than the fluid system used in the oil industry. Regarding VE applied to CO_2 storage, two conditions are established: a large aspect ratio (Figure 4.1: Horizontal versus vertical usually is greater than 1000) and gravity-capillarity equilibrium (zero flow perpendicular to the aquifer plane). VE can be considered a special case of the more general Dupuit approximation (*Bear*, 1979).

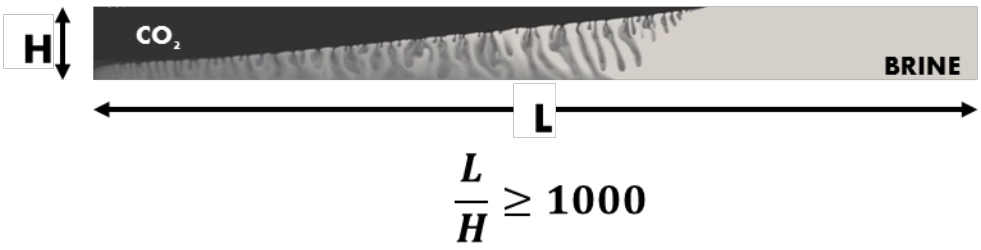

Figure 4.1: Large aspect ratio between thickness and length of a common reservoir for GCS.

The interest of the development of VE models oriented to simulation of CO_2 storage in the large-scale arises from the need to perform multiple simulations that would be required for risk analysis (*Wildenborg et al.*, 2005; *Oladyshkin et al.*, 2011).

Also, it could be an efficient computational alternative to classic modeling approach (as the standard numerical methods collected in section 3.1, i.e. *White and Oostrom*, 1997; *K. Pruess*, 1999; *Olivella et al.*, 1996; *Flemisch et al.*, 2011; *Wheeler et al.*, 2001), gaining in some processes qualitative and quantitative precision. In addition, semi-analytical methods have been increasingly developed in the past years (*Nordbotten et al.*, 2004, 2005a,b, 2009). These methods are oriented to incorporate different simplifying assumptions and upscaling techniques that are appropiate for typical CO_2 sequestration systems (*Hesse et al.*, 2009; *Dentz and Tartakovsky*, 2008), as it was explained in section 3.3.

Other recent studies have integrated these analytical and semi-analytical solutions into numerical tools, usually assuming VE, to model the injection zone with accuracy without having to renounce to a large scale simulation as a result. One of the most noteworthy studies is from *Gasda* (*Gasda et al.*, 2009, 2011) due to its scale range of applicability (*Møll Nilsen et al.*, 2015). *Gasda et al.* (2009) models were applied to the injection stage and to the early times after the injection stop. They assessed leakage risk through the caprock fracture, fault and abandoned wells. In this paper, VE with macroscopic sharp interface is assumed. It solved numerically in a coarse grid embedding in the sink/source points a sub-scale, in which an analytical method deals with the wellbore flow.

Further processes have been added, including the effect of capillary fringe (*Nordbotten and Dahle*, 2011) or taking into account the convective-dissolution process during the postinjection (*Gasda et al.*, 2011) in order to cover successfully the injection stage and the post injection stage (*Gasda et al.*, 2012). Afterward, it has been included other studies: analysis of the hysteresis in the VE (*Doster et al.*, 2012), the application into a multi-layered reservoir (*Guo et al.*, 2014) and the inclusion of compressible CO_2 into the vertically averaged equations (*Andersen et al.*, 2014). Lately, an open-source software which employs VE to study the long-term storage of the CO2 have been developed (*Møll Nilsen et al.*, 2015).

The following includes the vertical equilibrium governing equations for compressible multiphase flow based on Gasda 2009. We assume abrupt interface between CO_2 and brine and thermodynamic equilibrium in the vertical. Also we do not consider imbibition process or capillarity effects. To develop the equations, we begin plotting a scheme from Figures 4.1 which performs the three-dimensional system of CO_2 and brine within a reservoir of thickness H (Figure 4.2).

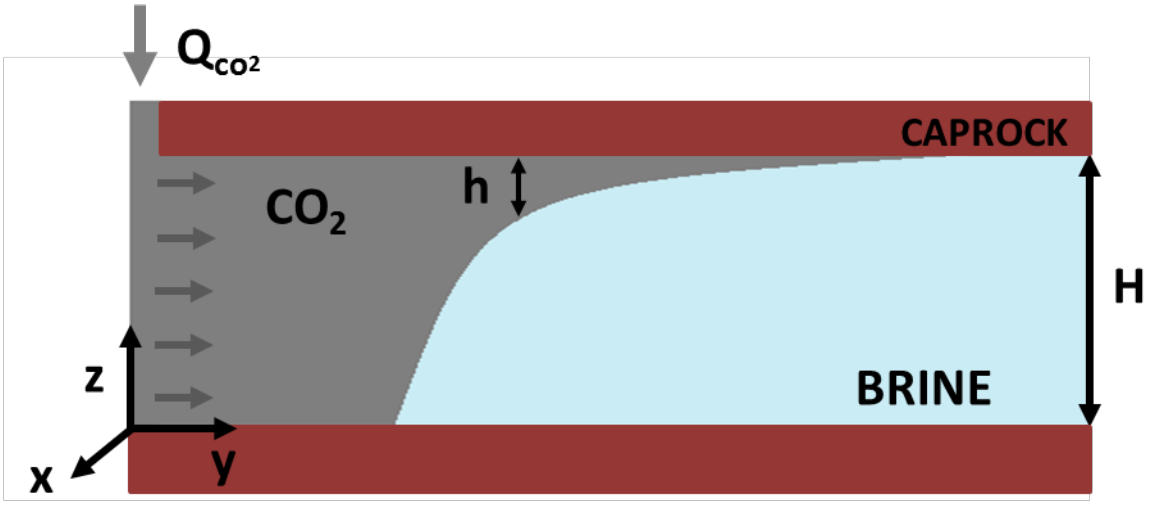

Figure 4.2 *Scheme of vertically averaged CO_2-brine system. Z zero-coordinate at the bottom of the aquifer.*

If we assume hydrostatic equilibrium in the z-direction, the vertical distribution of pressure is given by:

$$P(x,y,z) = P_z(x,y) + \rho_n g(H - z) \qquad if \;\; H < z \le h$$

$$P(x,y,z) = P_z(x,y) + \rho_n gh + \rho_w g(H - h - z) \qquad if \;\; h < z \le 0 \qquad \text{Eq. 4.1}$$

Where, P_z is the pressure on the top of the aquifer, ρ_n and ρ_w are density of the CO_2 and density of brine respectively, and g is gravity. Moreover, if we consider the residual brine saturation S_{wr} in the aquifer, the vertical distribution of phase saturations (S_n for CO_2 and S_w for brine) are:

$$\bar{S}_n = \frac{h}{H}(1 - S_{rw}) \qquad if \;\; H < z \le h \qquad \text{Eq. 4.2}$$

$$\bar{S}_n = \frac{H-h}{H} + S_{rw}\frac{h}{H} = \frac{H-h(1-S_{rw})}{H} \qquad if \;\; h < z \le 0$$

Once derived state variable distributions of our system, we integrate from bottom to top of the aquifer the basic balance equation for flow of each phase α in the system:

$$\frac{\partial}{\partial t}\left[\int_0^H S_\alpha \rho_\alpha \phi dz\right] + \nabla \cdot \left[\int_0^H q_\alpha \rho_\alpha dz\right] = \left[\int_0^H F_\alpha \rho_\alpha dz\right] \qquad \text{Eq. 4.3}$$

Where α is *n* (non-wetting phase is the CO_2) and *w* (wetting phase is the brine), S_α is the phase saturation, Ø is the porosity and F_α is the volumetric phase sink/source. Developing each term of the balance equation, and dividing by density, we get volume conservation equations of each phase:

- Non-wetting phase (CO_2)

$$\phi(1-S_{wr})h\beta_{n,m}\frac{\partial P_z}{\partial t} + \phi(1-S_{wr})\frac{\partial h}{\partial t} = -\nabla \cdot \left[-\frac{H\bar{k}_{rn}k}{\mu_n}\left(\nabla P_z + \rho_n g \nabla H\right)\right] + F_n \qquad \text{Eq. 4.4}$$

- Wetting phase (brine)

$$\phi(H-h)\beta_{w,m}\frac{\partial P_z}{\partial t} + \phi(1-S_{wr})\frac{\partial (H-h)}{\partial t} = -\nabla \cdot \left[-\frac{H\bar{k}_{rw}k}{\mu_w}\left(\nabla P_z - (\rho_w - \rho_n)g\nabla h + \rho_w g \nabla H\right)\right] + F_w \qquad \text{Eq. 4.5}$$

Where $\beta_{n,m}$, $\beta_{w,m}$, μ_n and μ_w are the vertically-averaged bulk compressibility and viscosities of CO_2 and brine, respectively, and k is the vertically-averaged intrinsic permeability. In order to simplify the effective parameters of our system, we define mobilities (λ_w, λ_n) and fractional flow (f_n, f_w)of each phases as:

$$\bar{\lambda}_n = \frac{\bar{k}_{rn}}{\mu_n} = \frac{(1-S_{rw})\frac{h}{H}}{\mu_n} = \frac{(1-S_{rw})h}{H\mu_n} \qquad \bar{\lambda}_w = \frac{\bar{k}_{rw}}{\mu_w} = \frac{\frac{H-h}{H}}{\mu_w} = \frac{(H-h)}{H\mu_w}$$

$$\bar{f}_n = \frac{\bar{\lambda}_n}{\bar{\lambda}_n + \bar{\lambda}_w} = \frac{\frac{(1-S_{rw})h}{H\mu_n}}{\frac{(1-S_{rw})h}{H\mu_n} + \frac{(H-h)}{H\mu_w}} \qquad \bar{f}_w = \frac{\bar{\lambda}_w}{\bar{\lambda}_n + \bar{\lambda}_w} = \frac{\frac{(H-h)}{H\mu_w}}{\frac{(1-S_{rw})h}{H\mu_n} + \frac{(H-h)}{H\mu_w}} \qquad \text{Eq. 4.6}$$

Finally, we pose the vertical averaged multiphase flow by a set of equations formed by the sum of phases (sum of Eq. 4.4 and Eq. 4.5) and the non-wetting equation (Eq. 4.4):

- Sum of phases ("pressure equation"):

$$\phi(\beta_{w,m}(1-S_{wr})h+\beta_{n,m}(H-h))\frac{\partial P_z}{\partial t}= \\ =\nabla\cdot\left[Hk\left(\lambda\nabla P_z+(\rho_n\bar{\lambda}_n+\rho_w\bar{\lambda}_w)g\nabla H-\bar{\lambda}_w(\rho_n-\rho_w)g\nabla h\right)\right]+F_n+F_w \quad \text{Eq. 4.7}$$

- Non-wetting phase ("height transport equation"):

$$\phi\beta_{n,m}(1-S_{wr})h\frac{\partial P_z}{\partial t}+\phi(1-S_{wr})\frac{\partial h}{\partial t}= \\ =\nabla\cdot\left[-\bar{f}_n(\bar{q}_n+\bar{q}_w)-Hk[(\bar{\lambda}_n(\rho_n(\bar{f}_n-1)+\rho_w\bar{f}_w)g\nabla H)-\bar{\lambda}_n\bar{f}_w(\rho_n-\rho_w)g\nabla h\right]+F_n \quad \text{Eq. 4.8}$$

This set of equation is posed to solve by an IMPES numerical resolution. This means that the "pressure" equation (Eq. 4.7) is solved implicitly and the transport of "height" (saturation) equation (Eq. 4.8) is solved explicitly. The transport of heights equation could need the use of a suitable technique for advective dominated equations.

5. Basin-scale storage capacity estimation workflow

5.1 Basin-scale capacity estimation approach

This evaluation of storage potential of a given site requires modeling of the long-term fate of the injected CO_2 and analyzing the storage capacity. We consider the capacity to be limited by both the injection pressure and the up-dip migration distance. For a given set of reservoir properties, which of the two limiting factors is the dominant one is unknown a priori. Reliable, efficient, basin-scale models both for pressure buildup and for CO_2 transport are needed. However, it is computationally demanding to run multiple 3D basin-scale numerical simulations, especially when parameter sensitivity and uncertainty need to be evaluated or multiple injection scenarios need to be tested. To this end, we propose a modeling procedure as outlined in **Figure. 5.1** to minimize the use of full 3D numerical simulations. We first apply (semi-)analytical solutions (see 3.3) for pressure buildup to determine maximum allowable injection rate (for a fixed injection period) and evaluate its sensitivity to various reservoir parameters. This provides a fast estimation of the pressure-limited capacity and can easily be applied to test different injection scenarios. We then model the injection and migration of CO_2 with the estimated maximum allowable injection rate using numerical models that allow inclusion of more geological detail and variability than the semi-analytical models. The numerical simulations are performed based on a TOUGH2-ECO2N model and a sharp-interface vertical equilibrium (VE) model. Through numerical simulations, the long-term fate of injected CO_2 is analyzed. The two numerical models are also compared in terms of their predictions of pressure buildup and plume migration.

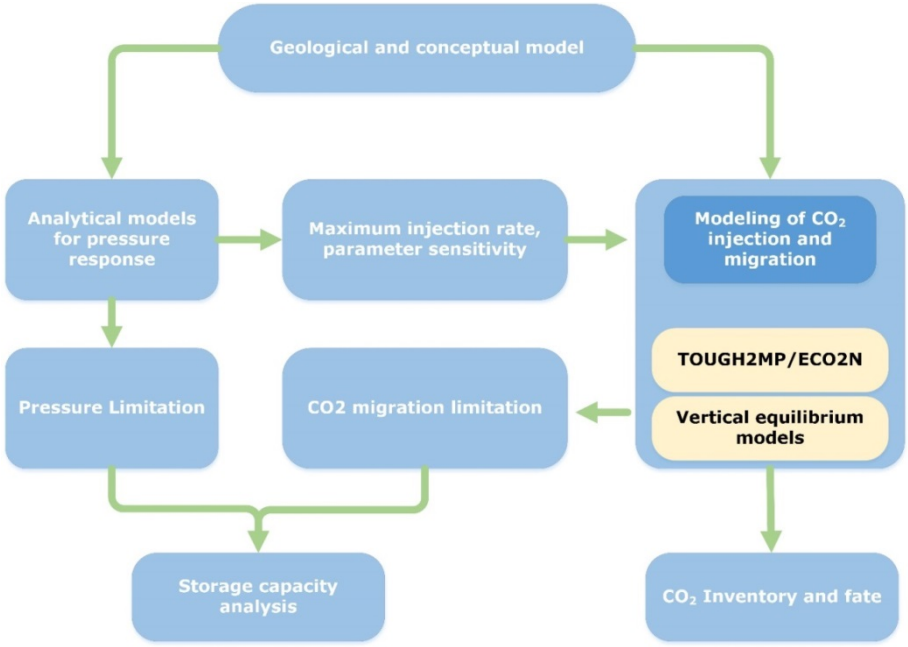

Figure 5.1: Basin-scale storage capacity estimation workflow.

6. Applications

6.1 Injection strategies (IIT and EWRE)

6.1.1 Introduction

The efficiency of CO_2 spreading and trapping in the formation is an important aspect of managing large scale sequestration projects. The location of the injection wells, their number and distribution, as well as their inclination are factors which have an effect on the spreading but once a decision regarding these factors has been taken it cannot be modified. Injection strategies remain as the only dynamic site management techniques.

This investigation deals with the effect of injection strategies on spreading via simulations. The following strategies have been studied:

1. Effect of temperature of injected CO_2.
2. Effect of intermittent injection of CO_2:
3. Effect of brine injection.
   a. Injection of water (brine) between periods of CO_2 injection.
   b. Injection of water (brine) in the upper portion of the reservoir between periods of CO_2 injection, or simultaneously with CO_2 injection.

6.1.2 Software

The software used is PFLOTRAN, included in section 3.1.

6.1.3 Geometry and grid

6.1.3.1 Geometry

The computational domain consists of a $10km \times 3km \times 50m$ rectangular box. Since the injection point is located on the $10km \times 50m$ face, the results apply to a $10km \times 6km$ domain (see 6.1). The domain is slightly inclined with respect to the larger horizontal direction, the slope equals 20m over 10km. The injection well is located 6km away from the downwards direction, between elevations 12m and 27m.

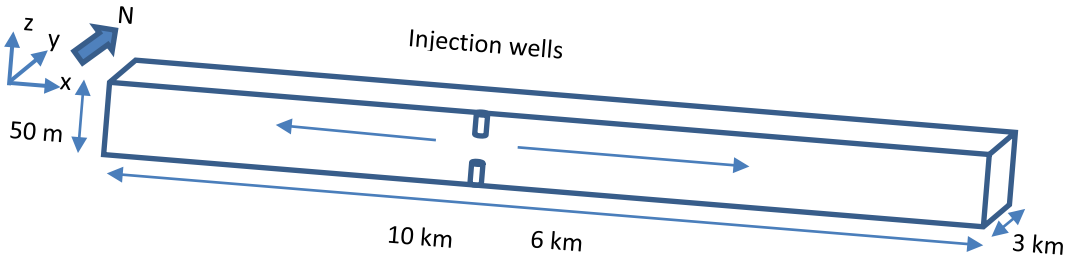

Figure 6.1: The computational domain and location of the injection wells.

6.1.3.2 Grid

The grid consists of 37,750 cells with varying density along the horizontal directions and 10 fixed width layers across the vertical direction.

6.1.4 Initial and boundary conditions

Boundary conditions: Impervious bottom and caprock faces. The $10km \times 50m$ face which contains the injection well cells is a symmetry boundary and the opposite face is impervious as well. The $3km \times 50m$ faces are open with Dirichlet pressure and temperature conditions.

Initial conditions: The bottom face pressure varies between 148 bar at the upwards end and 150 bar at the downwards end. The vertical hydrostatic pressure along the vertical direction has been calculated via an initial simulation without any injection during 6months. As a result of the inclination a uniform water flow is developed. The prevailing formation temperature was 67^0C.

6.1.5 Simulation details

porosity	Effective permeability – Van-Genuchten Mualem	tortuosity	Diffusion coef.
0.25	$\alpha = 1.5 * 10^{-4}$, $\lambda = 0.763$	0.1	liquid $1 * 10^{-9} \frac{m^2}{s}$, Gas $2.1 * 10^{-5} \frac{m^2}{s}$

Table 6.1 Simulation parameters.

6.1.6 Description and Results

6.1.6.1 Effect of injection temperature

Simulations with two different injection temperatures 30°C and 67°C have been carried on. The mass flow rate has been 200,000 ton/year. The total Duration of the simulation was 20 years, out of which co2 has been injected for the initial 9.5 years. The resulting near well pressure values was compared and the difference was found to be insignificant (Figure 6.2). Therefore this direction has not been pursued any further.

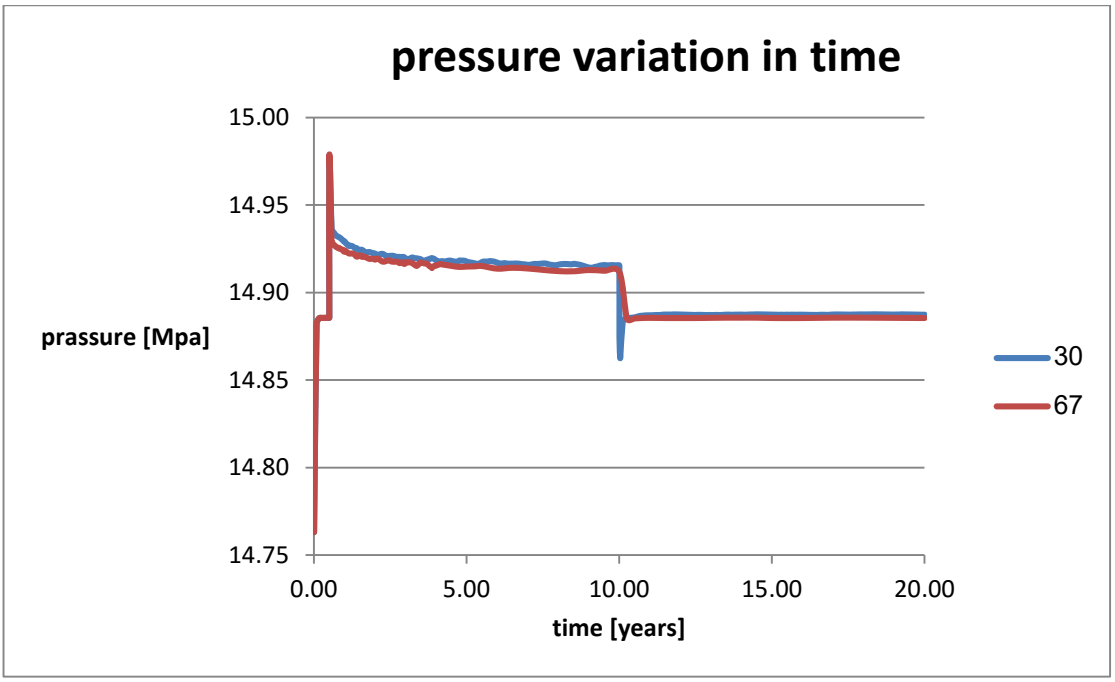

Figure 6.2: Effect of injection temperature on near well pressure.

6.1.6.2 Effect of intermittent (alternating injection temperature) injection

Three modes of injection have been compared:

I: Injecting intermittently CO_2 at 20°C for 3 months and then 60°C for 3 months. Total time 5 years.

II: Continuous injection at 20°C for 5 years

III: Continuous injection at 60°C for 5 years.

The mass flow rate has been 10^6 ton/year.

The following Figure 6.3 shows the difference of the CO_2 distributions between the different strategies after at the end of the injection period.

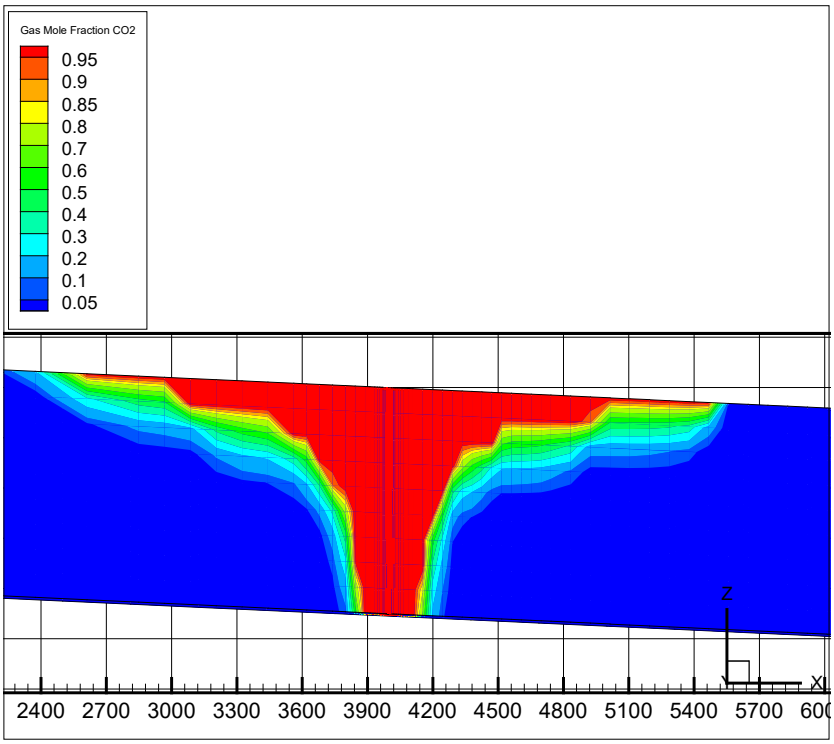

Figure 6.3: Effect of intermittent injection mode on CO_2 distribution.

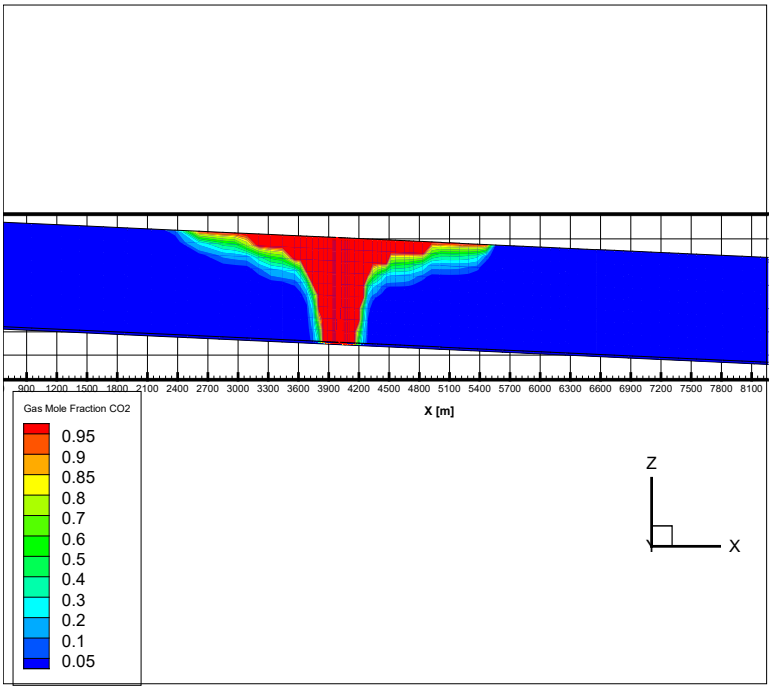

Figure 6.4 Effect of constant 20^{0}C injection mode on CO_2 distribution.

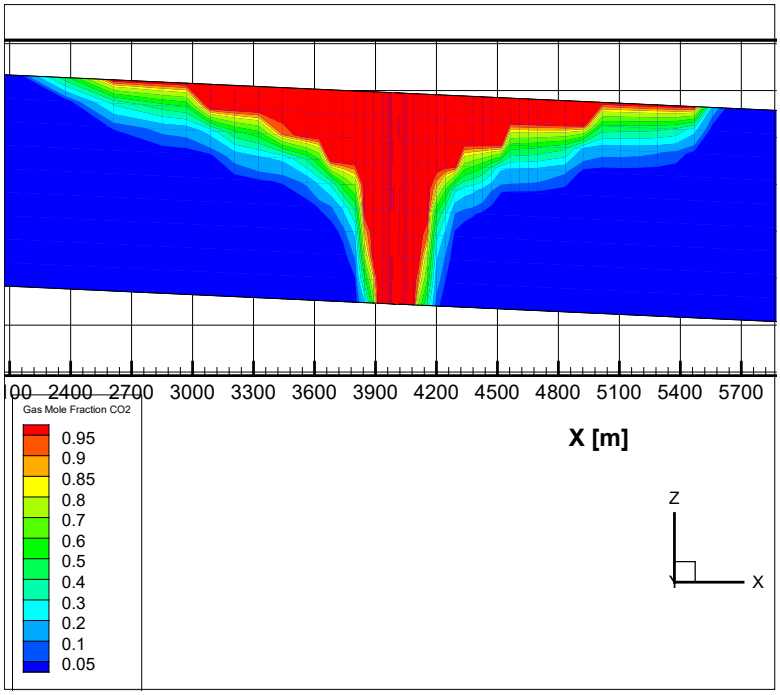

Figure 6.5: Effect of constant 60^{0}C injection mode on CO_2 distribution.

6.1.7 Conclusions

1. There is almost no difference in the time dependence of the near-well pressure curves between the two temperature values. This is an unexpected conclusion and we intend to examine and repeat this case carefully, as the result may be a consequence of the specific chosen aquifer inclination on flow in the aquifer. Something may also be wrong with the use of the software.

2. A difference in CO_2 spatial saturation distribution could be seen. The constant high temperature simulation presents the largest saturated area, while the constant low temperature simulation shows the smallest one, with the alternation simulation's area between the two.

6.2 Geomechanical response (IMPCOL)

6.2.1 Modelling Goals and Advances

One of the objectives of TRUST has been to extend and validate the ICGT in handling coupled thermo-hydro-mechanical deformation of a poro-elastic reservoir and caprock during CO_2 sequestration. In particular, the goal has been to investigate the possible effects on caprock integrity of temperature contrast during injection. As of today, all necessary extensions to the ICGT have been implemented, and the first field-scale simulation has been undertaken. Three-dimensional simulations will evaluate thermo-poro-elastic effects of CO_2 injection on the possible propagation and reactivation of existing fracture networks and faults, and the possible formation of new damage areas, with specific focus on features that lie at the caprock/reservoir interface. A new set of finite elements, isoparametric quadratic quarter point tetrahedra, has been developed and published (*Nejati et al.,* 2015a). The advances of the first year, on the development of a novel unstructured mesh stress intensity factor disk integration method have now also been published (*Nejati et al*., 2015b). IMPCOL has made other significant improvements to its geomechanics engine, including the automatic loading of material interfaces, which now allows the rapid loading of geological models. This has allowed creating and loading geometric field-scale models based on the UU publication by *Figueiredo et al.* (2015). Two field-scale geometric models of Heletz have now been created (see Fig. 6.6), and these can be automatically meshed and loaded into the IC Geomechanics Toolkit. Model boundary conditions and properties have been defined based on UU publications (resulting from the first period of TRUST) and are used as input to simulations. The validation of a novel friction model to capture friction effects on caprock integrity is underway. The development of an isotropic damage model to complement secondary, small-scale damage to the caprock is also underway (*Defoort et al*., 2015). Work is also currently underway on ensuring that large system numerical solutions converge appropriately, and on analysing the effect of initial conditions on stability. Stability is being evaluated in the context of large-scale, long-term simulations, in line with the objectives of the work package. Next steps include sensitivity analysis of the geomechanical deformation of Heletz in the context of long-term storage, with emphasis of caprock integrity. Further numerical experiments comparing modelling results to reports by *Fagerlund et al*. (2013) are also planned.

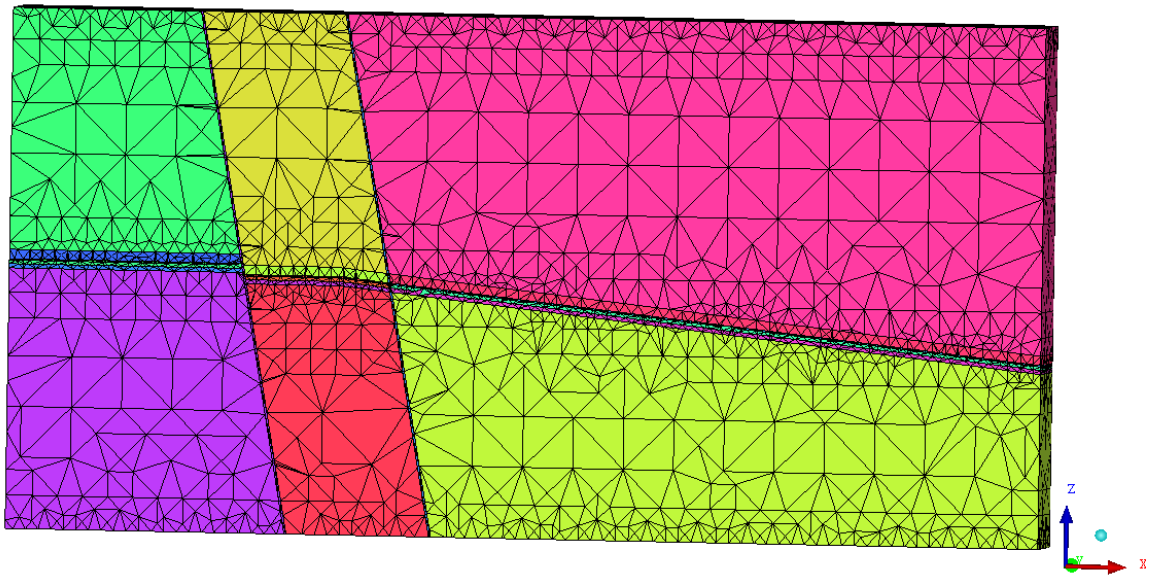

Figure 6.6: First Heletz dataset, automatically loaded and meshed during the simulation. The model is three dimensional, and is 5000 × 2500 × 400 m, a second thinner 40m width model was also built for comparison purposes. The horizontal section comprises four layers: dolomite, reservoir (upscaled 'AWK' layers as in *Figueiredo et al*. 2015), limestone and shale, the overburden and basement are assumed to be limestone. Two faults segment the reservoir into three compartments.

6.2.2 THM Coupling

During the first part of the TRUST project, IMPCOL developed an extension to the finite-element-based methodology for modelling thermo-poro-elastic geomechanical deformation, incorporating flow within the fractures, including leak-off terms to model fluid transfer between fracture and matrix that make use of pressure gradients within the matrix. The developed approach is based on the fully coupled method proposed by *Zimmerman* (2000). The governing equation for heat transfer through rock skeleton, matrix fluid and fracture fluid is modelled by combining Fourier's law with energy conservation for each entity (*e.g*. *Gelet et al*., 2012). The balance of energy accounts for the flux of thermal energy due to conduction, and the rate of entropy for solid and fluid, the rate of energy exchange between solid and fluid, as well as the rate in energy due to mass transfer and forced convection in the fluid. Fluid flow through the matrix is modelled using Darcy's law, while flow through the fracture is assumed to be laminar. Thermal transfer is modelled through both matrix and fractures. A set of virtual elements duplicates the nodes at the fracture-matrix interface in order to keep track of the fluid pressure of the matrix and fracture at the interface. A leak-off function is defined as a function of the fluid pressure gradient, and governs fluid flow through the fracture-matrix interface. A thorough validation of the geomechanical thermal components of the model is underway (see Fig. 6.7).

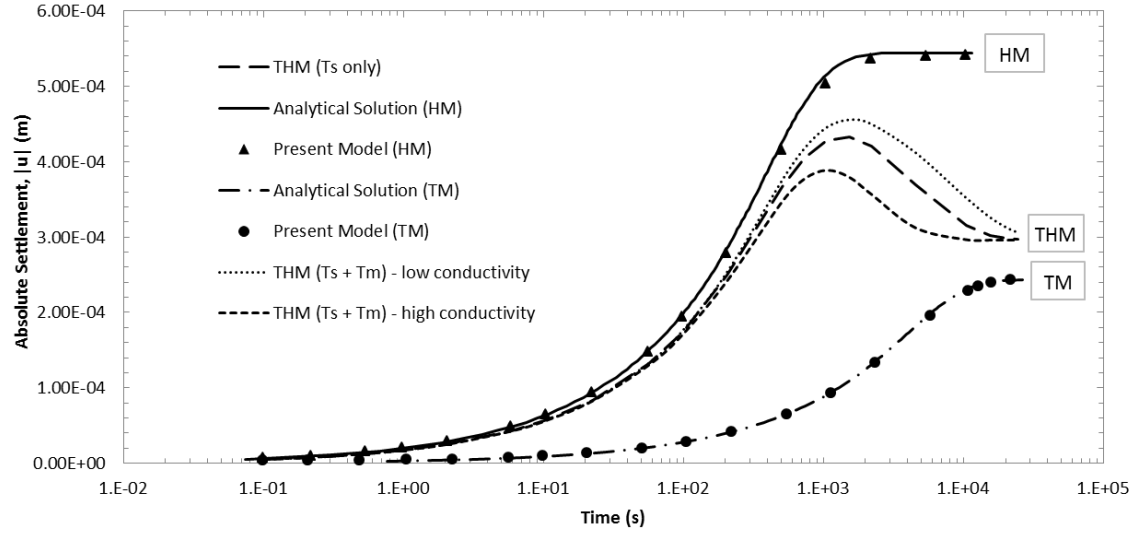

Figure 6.7: Thermo-poro-elastic validation of the coupling in the ICGT. Numerical results are depicted as points and triangles; analytical solutions are depicted as lines.

6.2.3 Validation against Field-Scale Goldeneye Data

IMPCOL has also conducted its first field-scale validation study using publicly available data of the Goldeneye field. These have been tested in the context of published field-based data and numerical experiments of the production and subsequent CO_2 sequestration in Goldeneye. Simulations of oil depletion were performed, to compare numerical results against actual field data. Figure 6.8 shows the displacement field at the end of oil production over five years, with well pressure decreasing linearly with time, by 10 MPa. The 50×20×8 km model (577k tetrahedral elements) contains eleven geo-physically mapped faults in the Rødby caprock, and models poro-elastic effects of the depletion on the displacement of the seabed surface. Most displacement occurs around the fault planes, which in this case are assumed to be of vertical orientation and have zero friction. The displacement at the seabed and at the top of the reservoir is predicted to be 11.6 cm and 7.0 cm (see Figs. 6.9 and 6.10), comparable to the actual field measurements reported by Shell: 8.9 cm and 4.6 cm (UKCCS, 2011). Resulting fluid pressure values during and at the end of production are also within the expected ranges. As opposed to defining faults as weakness zones, the IMPCOL simulator allows fault planes to be represented as explicit and discrete discontinuity planes. Therefore, the possible reactivation of these faults can be robustly assessed using well-established energy criteria for fault propagation. Developed methods for the accurate computation of stress intensity factors (reported in the previous period of TRUST) can be directly applied to measure modal growth energy concentrations at the tips of the defined faults, which indicate the tendency of fault growth during the geomechanical deformation of the field. These take into account both fluid and solid deformation simultaneously. In the case of Goldeneye, modest growth is predicted, including sideways growth during depletion in tensile mode, as well as shear growth towards the basement. After injection, during pressure stabilization, stresses redistribute and shear growth is predicted in the upward direction. Simulation of injection tests is currently underway. A publication reporting these results in detail is being prepared.

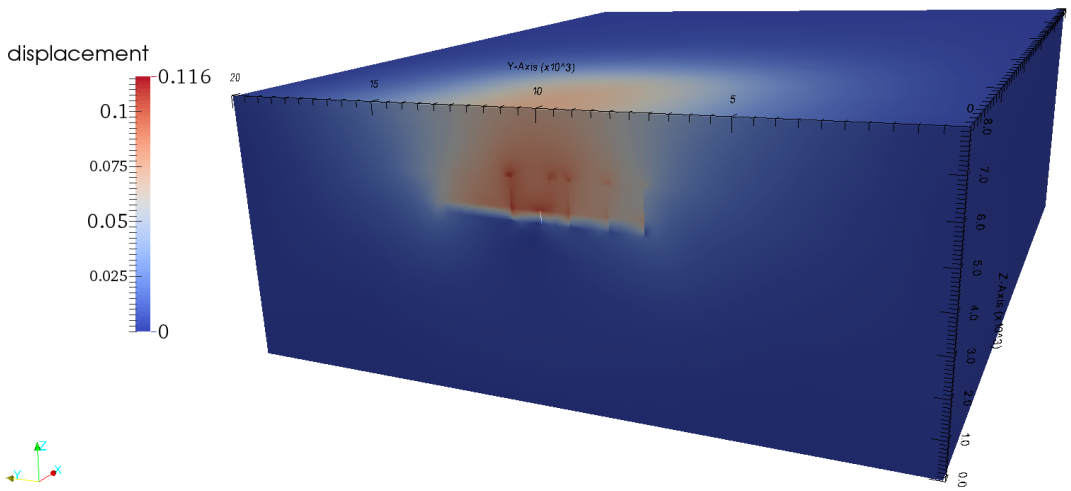

Figure 6.8: Field-scale validation using North Sea Goldeneye field data and measured subsidence data.

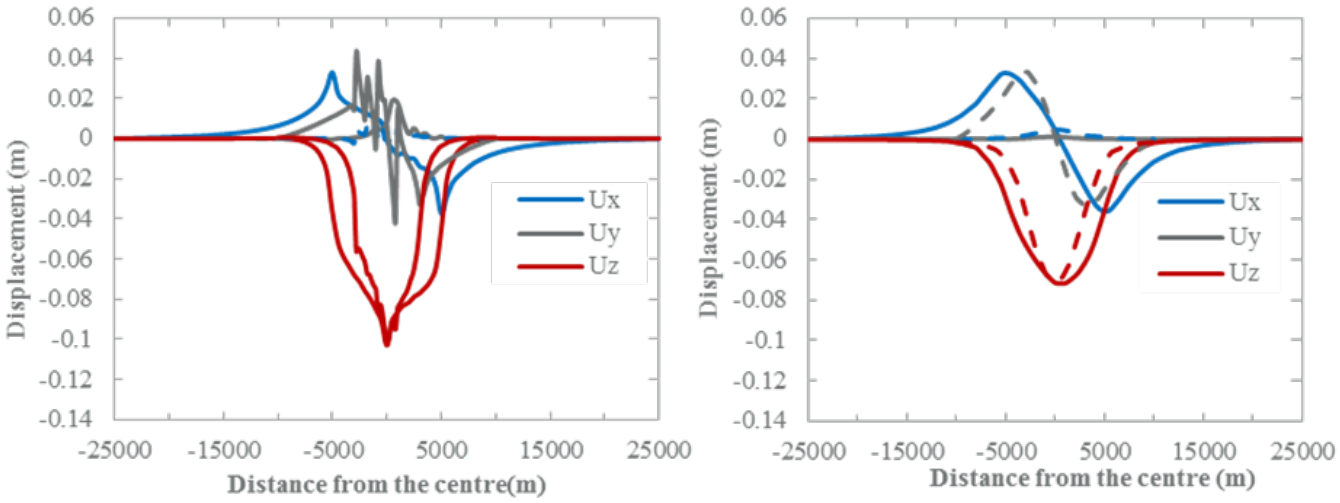

(a) (b)

Figure 6.9: Displacement (U) in the x, y, and z directions along a line at (a) the top of the reservoir, and (b) at the top of the model (on the seabed). In (a), the oscillations correspond to the presence of faults in the caprock. Maximum displacements are in good agreement with field measurements.

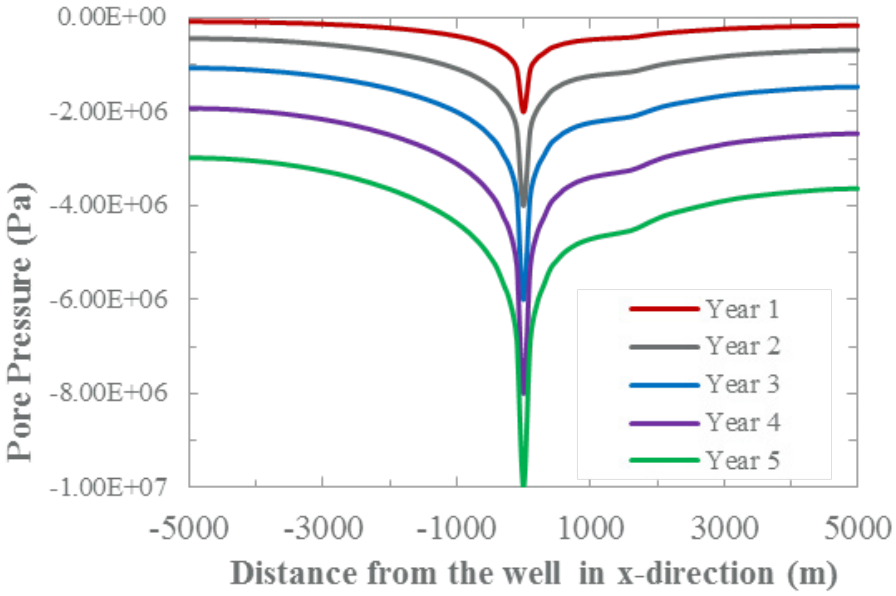

Figure 6.10: Pore pressure evolution during the five-year depletion. This depletion exercise is a numerical test of our geomechanics simulation tool in the context of poro-elastic deformation, which can be readily validated against actual measured data from the field (UKCCS, 2011).

7. References

Andersen, O., S. E. Gasda, and H. M. Nilsen (2014), Vertically averaged equations with variable density for co2 flow in porous media, *Transport in PorousMedia*, *107*(1), 95–127, doi:10.1007/s11242-014-0427-z.

Bauer, S., et al. (2012), Modeling, parameterization and evaluation of monitoring methods for CO2 storage in deep saline formations: the CO2-mopa project, *Environmental Earth Sciences*, *67*(2), 351–367, doi:10.1007/ s12665-012-1707-y.

Bakker, M. (2003), A dupuit formulation for modeling seawater intrusion in regional aquifer systems, *Water Resour. Res.*, *39*(5), n/a–n/a, doi:10.1029/2002wr001710.

Bear, J. (1979), *Hydraulics of groundwater*,McGraw-Hill International Book Co.

Bear, J. (1999), Mathematical modeling of seawater intrusion, *Seawater Intrusion into Coastal Aquifers. Kluwer Academic Publications*, pp. 127–161.

Class, H., et al. (2009), A benchmark study on problems related to CO2 storage in geologic formations, *Computational Geosciences*, *13*(4), 409–434, doi:10.1007/s10596-009-9146-x.

Coats, K., R. Nielsen, M. H. Terhune, and A.Weber (1967), Simulation of three-dimensional, two-phase flow in oil and gas reservoirs, *Society of Petroleum Engineers Journal*, *7*(04), 377–388, doi:10.2118/1961-pa.

Coats, K., J. Dempsey, and J. Henderson (1971), The use of vertical equilibrium in two-dimensional simulation of three-dimensional reservoir performance, *Society of Petroleum Engineers Journal*, *11*(01), 63–71, doi:10.2118/2797-pa.

Cook, N. (1992), Natural joints in rock: Mechanical, hydraulic and seismic behaviour and properties under normal stress, *International Journal of Rock*

Defoort, T., Salimzadeh, S., Paluszny, A., Zimmerman, R. W. (2015) A finite element geomechanical study of the brittle failure of a caprock due to deflation. *49th US Rock Mechanics Symposium* (ARMA), San Francisco, 28 June - 1 July, 2015.

Dentz, M., and D. M. Tartakovsky (2008), Abrupt-interface solution for carbon dioxide injection into porous media,*Transport in PorousMedia*, *79*(1), 15–27, doi:10.1007/s11242-008-9268-y.

Dietz, D. (1953), A theoretical approach to the problem of encroaching and by-passing edge water, *Proc. Akad. Van Wetenschappen*, *56*, 83–92.

Doster, F., J. M. Nordbotten, and M. A. Celia (2012), Hysteretic upscaled constitutive relationships for vertically integrated porous media flow, *Computing and Visualization in Science*, *15*(4), 147–161, doi:10.1007/s00791-013-0206-3.

Fagerlund, F., Niemi, A., Bensabat, J., Shtivelman V. (2013) Design of a two-well field test to determine in situ residual and dissolution trapping of CO2 applied to the Heletz CO2 injection site. *Int. J. Greenhouse Gas Control*, 19, pp. 642-651.

Figueiredo, B., Tsang, C.-F., Rutqvist J., Niemi A. (2015) Coupled hydro-mechanical processes and fault reactivation induced by CO2 injection in a three layer storage formation. *Int. J. Greenhouse Gas Control*, 39, pp. 432-448.

Flemisch, B., Fritz, J., Helmig, R., Niessner, J., Wohlmuth, B.: DUMUX: amulti-scale multi-physics toolbox for flow and transport processes in porous media. In: Ibrahimbegovic, A., Dias, F. (eds.) ECCOMAS Thematic Conference on Multiscale Computational Methods for Solids and Fluids, Cachan, 28–30 November 2007.

Gasda, S. E., J. M. Nordbotten, and M. A. Celia (2009), Vertical equilibrium with sub-scale analytical methods for geological CO2 sequestration, *Computational Geosciences*, *13*(4), 469–481, doi:10.1007/s10596-009-9138-x.

Gasda, S. E., J. M.Nordbotten, and M. A. Celia (2011), Vertically averaged approaches for co 2 migration with solubility trapping,*Water Resour. Res.*, *47*(5), doi:10.1029/2010wr009075.

García-Rios, M., L. Luquot, J. M. Soler, and J. Cama (2013), Laboratory-scale interaction between CO2-rich brine and reservoir rocks (limestone and sandstone), *Procedia Earth and Planetary Science*, *7*, 109–112, doi:10.1016/j.proeps.2013.03.013.

Gelet, R., Loret, B., Khalili, N. (2012) A thermo-hydro-mechanical coupled model in local thermal non-equilibrium for fractured HDR reservoir with double porosity. *J. Geophys. Res.,* 117*,* B07205.

GHS (Hydrogeology Group) Spreadsheet with the semianalytical solution for CO2 injection. http://www.h2ogeo.upc.es/publicaciones/2011/Semianalytical_solution.xlsx (2012)

Guo, B., K. W. Bandilla, E. Keilegavlen, F. Doster, and M. A. Celia (2014), Application of vertically-integrated models with subscale vertical dynamics to field sites for CO2 Sequestration, *Energy Procedia*, *63*, 3523–3531, doi:10.1016/ j.egypro.2014.11.381.

Helmig, R., B. Flemisch, M.Wolff, A. Ebigbo, and H. Class (2013),Model coupling for multiphase flowin porous media, *Advances inWater Resources*, *51*, 52–66, doi:10.1016/j.advwatres.2012.07.003.

Hesse, M., F. Orr Jr., and H. Tchelepi (2009), Gravity currents with residual trapping, *Energy Procedia*, *1*(1), 3275–3281,doi:10.1016/j.egypro.2009.02.113.

Hidalgo, J. J., C. W. MacMinn, and R. Juanes (2013), Dynamics of convective dissolution from a migrating current of carbon dioxide, *Advances inWater Resources*, *62*, 511–519, doi:10.1016/j.advwatres.2013.06.013.

Korbul, R. and A. Kaddour (1995), Sleipner vest co2 disposal—injection of removed co2 into the utsira formation, *Energy ConvManage, 36 (6–9), pp. 509–512*.

K. Pruess, G. M., H.C. Oldenburg (1999), *TOUGH2 User's Guide, Version 2.0,*, vol. Report LBNL-43134 p. 197 (pp), Lawrence Berkeley National Laboratory, Berkeley, California, USA.

Martin, J. C. (1958), Some mathematical aspects of two phase flow with application to flooding and gravity segregation, *Prod.Monthly*, *22*(6), 22–35.

Mathias S. A., J. G. Gluyas, G. J. González Martínez de Miguel, and S. A. Hosseini, "Role of partial miscibility on pressure buildup due to constant rate injection of CO_2 into closed and open brine aquifers," *Water Resources Research*, 2011.

Møll Nilsen, H., K.-A. Lie, and O. Andersen (2015a), Analysis of CO2 trapping capacities and long-term migration for geological formations in the norwegian north sea using mrst-co2lab, *Computers & Geosciences*, *79*, 15–26, doi: 10.1016/j.cageo.2015.03.001.

Møll Nilsen, H., K.-A. Lie, and O. Andersen (2015b), Analysis of CO2 trapping capacities and long-term migration for geological formations in the norwegian north sea using mrst-co2lab, *Computers & Geosciences*, *79*, 15–26, doi: 10.1016/j.cageo.2015.03.001.

Nejati, M., Paluszny, A., Zimmerman, R.W. (2015a) On the use of quarter-point tetrahedral finite elements in linear elastic fracture mechanics. *Eng. Fract. Mech.,* 144, pp. 194-221.

Nejati, M., Paluszny, A., Zimmerman, R.W. (2015b) A disk-shaped domain integral method for the computation of stress intensity factors using tetrahedral meshes. *Int. J. Solids Struct*., 69-70, pp. 230-251.

Nordbotten, J. M., and H. K.Dahle (2011), Impact of the capillary fringe in vertically integrated models for co 2 storage, *Water Resour. Res.*, *47*(2), doi:10.1029/2009wr008958.

Nordbotten, J. M., M. A. Celia, and S. Bachu (2004), Analytical solutions for leakage rates through abandoned wells, *Water Resour. Res.*, *40*(4), n/a–n/a, doi:10.1029/2003wr002997.

Nordbotten, J. M., M. A. Celia, S. Bachu, and H. K. Dahle (2005a), Semianalytical solution for co 2 leakage through an abandoned well, *Environ. Sci. Technol.*, *39*(2), 602–611, doi:10.1021/es035338i.

Nordbotten, J. M., M. A. Celia, and S. Bachu (2005b), Injection and storage of CO2 in deep saline aquifers: Analytical solution for CO2 plume evolution during injection, *Transport in Porous Media*, *58*(3), 339–360, doi: 10.1007/s11242-004-0670-9.

Oladyshkin, S., H. Class, R. Helmig, andW. Nowak (2011), An integrative approach to robust design and probabilistic risk assessment for CO2 storage in geological formations, *Computational Geosciences*, *15*(3), 565–577, doi:10.1007/s10596-011-9224-8.

Olivella, S., A. Gens, J. Carrera, and E. Alonso (1996), Numerical formulation for a simulator (code-bright) for the coupled analysis of saline media, *Engineering Computations*, *13*(7), 87–112, doi:10.1108/02644409610151575.

Palandri, J. L., R. J. Rosenbauer, and Y. K. Kharaka (2005), Ferric iron in sediments as a novel CO2 mineral trap: CO2–so2 reaction with hematite, *Applied Geochemistry*, *20*(11), 2038–2048, doi:10.1016/j.apgeochem.2005.06.005.

Parkhurst, D. L., C. Appelo, et al. (1999), User's guide to phreeqc (version 2): A computer program for speciation, batch-reaction, one-dimensional transport, and inverse geochemical calculations.

PFLOTRAN User Manual: A Massively Parallel Reactive Flow and Transport Model for Describing Surface and Subsurface Processes, Lichtner, Peter et al. Los Alamos National Laboratory, Report LA-UR-15_20403. January, 2015

Pool, M., J. Carrera, M. Dentz, J. J. Hidalgo, and E. Abarca (2011), Vertical average for modeling seawater intrusion, *Water Resour. Res.*, *47*(11), n/a–n/a, doi:10.1029/2011wr010447.

Rutqvist, J., Y.-S.Wu, C.-F. Tsang, and G. Bodvarsson (2002), A modeling approach for analysis of coupled multiphase fluid flow, heat transfer, and deformation in fractured porous rock, *International Journal of Rock Mechanics and Mining Sciences*, *39*(4), 429–442, doi:10.1016/s1365-1609(02)00022-9.

Schlumberger: Eclipse Technical Description 2007.1 (2007).

Sorek, S., V. Borisov, and A. Yakirevich (2001), A two-dimensional areal model for density dependent flow regime, *Transport in porous media*, *43*(1), 87–105.

Spycher, N., and K. Pruess (2009), A phase-partitioning model for CO2–brine mixtures at elevated temperatures and pressures: Application to CO2-enhanced geothermal systems, *Transport in Porous Media*, *82*(1), 173–196, doi:10.1007/s11242-009-9425-y.

Steefel, C. (2009), Crunchflow software for modeling multicomponent reactive flow and transport. user's manual, *Earth Sciences Division. Lawrence Berkeley, National Laboratory, Berkeley, CA. October*, pp. 12–91.

Taber, J. (1994.), A study of technical feasibility for the utilization of co2 for enhanced oil recovery. Riemer. The utilization of carbon dioxide from fossil fuel fired power stations., *Appendix B: IEA Greenhouse Gas R&D Programme, Cheltenham, UK;*.

Tian L., Z. Yang, B. Jung, S. Joodaki, M. Erlström, Q. Zhou, and A. Niemi (2015), Integrated simulations of CO_2 spreading and pressure response in the multilayer saline aquifer of Southwest Scania Site, Sweden. Greenhouse Gases: Science and Technology, in revision.

Vilarrasa, V., O. Silva, J. Carrera, and S. Olivella (2013), Liquid CO2 injection for geological storage in deep saline aquifers, *International Journal of Greenhouse Gas Control*, *14*, 84–96, doi:10.1016/j.ijggc.2013.01.015.

Walsh, J. (1981), Effect of pore pressure and confining pressure on fracture permeability, *International Journal of Rock Mechanics andMining Sciences & Geomechanics Abstracts*, *18*(5), 429–435, doi:10.1016/0148-9062(81)90006-1.

Wheeler, J., Wheeler, M.F., et al.: Integrated parallel and accurate reservoir simulator. Technical report, TICAM01-25,CSM, University of Texas at Austin (2001).

White, M.D., and M.Oostrom(1997), Stomp subsurface transport over multiple phases: Users guide, *Tech. rep.*, Pacific Northwest Lab., Richland,WA (United States).

Wildenborg, A., et al. (2005), Risk assessment methodology for CO2 Storage, *Carbon Dioxide Capture for Storage in Deep Geologic Formations*, p. 1293–1316, doi:10.1016/b978-008044570-0/50162-8.

UK Carbon Capture and Storage Demonstration Competition, UKCCS - KT - S7.19 - Shell – 004 Geomechanics Summary Report, ScottishPower CCS Consortium, April 2011.

Yang, Z., A. Niemi, L. Tian and M. Erlström (2013), Modelling of far-field pressure plumes for carbon dioxide sequestration. *Energy Procedia*, 40, 472-480.

Yang, Z., A. Niemi, L. Tian, S. Joodaki, and M. Erlström (2015), Modeling of pressure buildup and estimation of maximum injection rate for geological CO_2 storage at the South Scania site, Sweden, Greenhouse Gases: Science and Technology 5(3), 277-290.

Yang Z., L. Tian, B. Jung, S. Joodaki, F. Fagerlund, R. Pasquali, R. Vernon, N. O'Neill, and A. Niemi (2015), Assessing CO_2 storage capacity in the Dalders Monocline of the Baltic Sea Basin using dynamic models of varying complexity. International Journal of Greenhouse Gas Control, In Press.

Yang, Z., A. Niemi, L. Tian, S. Joodaki, and M. Erlström (2015), Modeling of pressure buildup and estimation of maximum injection rate for geological CO_2 storage at the South Scania site, Sweden, Greenhouse Gases: Science and Technology 5(3), 277-290.

Yortsos, Y. A theoretical analysis of vertical flow equilibrium *Transport in Porous Media, Kluwer Academic Publishers,* **1995***, 18*, 107-129.

Zimmerman, R.W. (2000) Coupling in poroelasticity and thermoelasticity. *Int. J. Rock Mech. Min. Sci.*, 37, pp. 79-87.